Characteristics of helium fragments produced in ^{28}Si emulsion interactions at 14.5 A GeV

G. Singh, A. Z. M. Ismail,* and P. L. Jain
High Energy Experimental Laboratory, Department of Physics, State University of New York at Buffalo, Buffalo, New York 14260
(Received 17 December 1990)

We report the measurements on partial production cross sections of the multiple helium fragments emitted in the interactions of ^{28}Si ions at 14.5 A GeV in nuclear emulsion. Interaction mean free paths of the helium fragments have been investigated on the basis of helium multiplicity and size of the target nucleus as a function of the distance from their production points. Multiplicity scaling in the produced helium fragments is also observed.

I. INTRODUCTION

From the last few years, emergence of heavy-ion accelerator facilities at Brookhaven National Laboratory (BNL) Alternating Gradient Synchrotron (AGS) and the CERN Super Proton Synchrotron (SPS) has opened up the possibilities of exploring new avenues in the fields of particle and nuclear physics at ultrarelativistic energies.[1] Most of the studies carried out have focused attention primarily on the search for a quark-gluon plasma which might be formed in central collisions. However, a number of other interesting aspects in physics can be studied in the peripheral collisions involving the heavy ions. As far as we know, no experiment is performed on the study of partial production cross sections and on the interaction mean free paths of the helium fragments at the AGS energies in nuclear emulsion prior to the present investigation. In this paper, we present the results on the partial production cross sections and the mean free paths of the helium fragments emerged in the interactions of ^{28}Si at 14.5 A GeV in nuclear emulsion as a function of the distance from their birth locations and also compare the present results with our previous findings[2–5] on helium particles produced at different energies. An attempt has also been made to check the validity of the helium multiplicity scaling at the AGS energies. In general, the detection of helium fragments is quite definite due to their distinctive grain density and, moreover, the use of electron-sensitive Fuji nuclear emulsion detectors allows an exclusive type of analysis on an event-by-event basis.

II. EXPERIMENTAL DETAILS

The present experiment (No. 847) was performed in a stack consisting of 24 Fuji nuclear research emulsion pellicles of dimensions $16\times10\times0.06$ cm^3, exposed horizontally to the 14.5 A GeV ^{28}Si ions at the BNL AGS. The beam flux was 3×10^3 ions/cm^2. In order to obtain an unbiased sample of events, an along-the-track scanning technique was employed and the pellicles were scanned on digitized stage microscopes under 100× magnification using oil immersion objectives. The primary tracks were picked up at a distance of 4 mm from the entrance edge of the pellicle and were carefully followed until they either interacted or escaped from the pellicle. In case the primary track interacted with the nuclei of emulsion, the following visual features of the event were recorded: N_b, the number of black tracks; N_g, the number of grey tracks; $N_h=N_b+N_g$, the number of heavy tracks from the target nucleus; n_s, the number of minimum ionizing shower tracks which included the number of singly charged projectile proton tracks; N_f, the number of projectile fragments (PF's) of charge $Z\geq2$. The charges of the PF's were determined by measuring the grain density, gap density, and by δ-ray counting as discussed in Ref. 2. Further details of the event classification can be found in Ref. 6.

By following 113.25 m of the primary track length, a total of 1003 events was observed, leading to a mean free path of ^{28}Si nuclei in emulsion $\lambda_{\rm tot}=11.29\pm0.36$ cm, which corresponds to the value of the total cross section, $\sigma_{\rm tot}=1121\pm34$ mb. Among 1003 primary events, 88 events were due to the electromagnetic dissociation (ED's) of the ^{28}Si projectile and the rest were due to the inelastic interactions. Experimental value of the mean free path for the latter class of events is $\lambda_{\rm inel}=12.38\pm0.41$ cm and that of the cross section, $\sigma_{\rm inel}=1023\pm34$ mb. Out of 915 inelastic events, 187 were central and the remaining 728 events were observed to be peripheral. Since our analysis pertains to the helium projectile fragments, we divided the inclusive distribution of the projectile fragments of charge $Z\geq2$ into two principal categories: (i) $\sigma_{n\alpha}$, where $n=1,\ldots,6$. This category of peripheral events is always accompanied by n helium fragments along with other fragments of charge $Z=1$ and $Z\geq3$. (ii) $\sigma_{0\alpha}$. This reaction channel consists of events with no helium fragments; however, the fragments of charge $Z=1$ and $Z\geq3$ are possible. In total, 525 peripheral events fulfilled the selection criterion of the former category (i) of events in which 934 helium fragments were observed. The general details of charge determination and of following the helium fragments in subsequent pellicles are discussed elsewhere.[3]

TABLE I. Partial production cross sections (in mb) for central (σ_C), peripheral (σ_P), and multiple alpha emission ($\sigma_{n\alpha}$) events. Figures given within the parentheses represent the percentile abundances.

Cross section	^{28}Si at 14.5A GeV	^{32}S at 200A GeV[a]
σ_C	209±15 (20.4)	233±15 (20.2)
σ_P	814±30 (79.6)	917±30 (79.8)
$\sigma_{n\alpha}$	587±26 (57.4)	636±25 (55.3)
$\sigma_{0\alpha}$	227±16 (22.2)	281±17 (24.5)
$\sigma_{1\alpha}$	300±18 (29.3)	345±19 (30.3)
$\sigma_{2\alpha}$	171±14 (16.7)	171±17 (14.9)
$\sigma_{3\alpha}$	69±9 (6.7)	81±9 (7.0)
$\sigma_{4\alpha}$	44±7 (4.3)	28±5 (2.4)
$\sigma_{5\alpha}$	3±2 (0.3)	8±3 (0.7)
$\sigma_{6\alpha}$	1±1 (0.1)	4±2 (0.3)

[a]Reference 5.

III. RESULTS

A. Partial production cross sections

In Table I, we present the results on the partial production cross sections for central (σ_C), peripheral (σ_P), and multiple helium ($\sigma_{n\alpha}$) events. Also given in this table are the results on the production cross sections for the ^{32}S-induced emulsion reactions at 200A GeV from the CERN SPS. It is interesting to point out that percentile abundances of all the reaction channels, except with 5α and 6α events, at the AGS and CERN energies are very close to each other. Consequently, the production cross sections for these classes of events are also approximately the same within their experimental errors and thus exhibit an energy-independent behavior. Discrepancy in the values of the partial cross sections for reaction channels with 5α and 6α emission may be due to low statistics for the ^{28}Si data.

B. Interaction mean free paths

In our former investigations[4,5] at Bevatron and CERN energies, we studied the variation of the mean free paths of the helium fragments emerged in emulsion-induced reactions as a function of the distances from their production points and found that they did not depend upon the helium multiplicity and the size of the target nuclei. In this section, we study the interaction mean free paths of projectile helium fragments emitted in ^{28}Si emulsion events at AGS energies (14.5A GeV) and, consequently, a track length of 80.15 m for the helium fragments was followed during which 344 secondary inelastic interactions were recorded. In Table II, we present the salient features of the primary peripheral events of ^{28}Si along with the mean free paths of the secondary helium tracks calculated for distances $L \leq 3$ cm and $L > 3$ cm on the basis of different helium multiplicity. The mean free paths are found to be independent of the distances considered. In Table III, we depict the overall characteristics of the primary and secondary inelastic events on the basis of different categories of the target nuclei in emulsion. One can observe from Table III that the overall values of the mean free paths do not seem to depend on the size of the target nucleus within their statistical errors.

We plot the variation of the mean free path (λ) as a function of the distance (L) from the vertex of the primary interactions in Figs. 1(a)–(d) for 1α, 2α, 3α, and 4α multiplicities, respectively. This parameter (λ) in different path lengths (L) is calculated by dividing the total track length followed in a particular path length by the number of inelastic helium interactions observed in that path length. It is obvious from Figs. 1(a)–(d) that the values of mean free paths do not depend upon the distance from their production point for different helium multiplicity events. These results are in agreement with our previous results at the CERN and Bevatron energies.[4,5]

We now investigate the dependences of mean free

TABLE II. Characteristics of primary inelastic interactions of the ^{28}Si beam having different helium multiplicities and the mean free paths of the helium fragments produced in the events.

	Primary information			Secondary information			
He multiplicity	No. of events	$\langle n_s \rangle$	$\langle N_h \rangle$	No. of events	Total track length followed (m)	λ (cm) $L \leq 3$ cm	$L > 3$ cm
1	268	22.7±1.4	8.0±0.5	92	24.12	27.94±5.38	25.50±3.16
2	153	20.3±1.6	7.2±0.6	115	26.74	19.09±2.88	25.83±3.07
3	61	17.1±2.2	7.9±1.0	67	14.26	20.39±4.16	21.78±3.32
4	39	13.8±2.2	3.7±0.6	62	13.24	22.49±5.16	20.86±3.18
4,5,6	43	13.4±2.0	3.8±0.6	70	15.03	21.95±4.68	21.25±3.07
All He	525	20.6±0.9	7.4±0.3	344	80.15	21.94±2.03	24.00±1.59

TABLE III. Characteristics of primary inelastic events of the ^{28}Si beam with different target nuclei of emulsion, having at least one helium fragment and the mean free paths of the helium fragments produced.

	Primary information			Secondary information			
Target	No. of events	$\langle n_s \rangle$	$\langle N_h \rangle$	No. of He tracks followed	Total track length (m)	No. of inelastic events	λ (cm)
Emulsion	525	20.6±0.9	7.4±0.3	934	80.15	344	23.30±1.2
H	109	12.2±1.2	0.4±0.03	211	17.64	77	22.91±2.6
CNO	242	17.6±1.1	4.1±0.3	454	40.54	164	24.72±1.9
AgBr	174	30.1±2.3	16.5±1.3	269	21.96	103	21.32±2.1

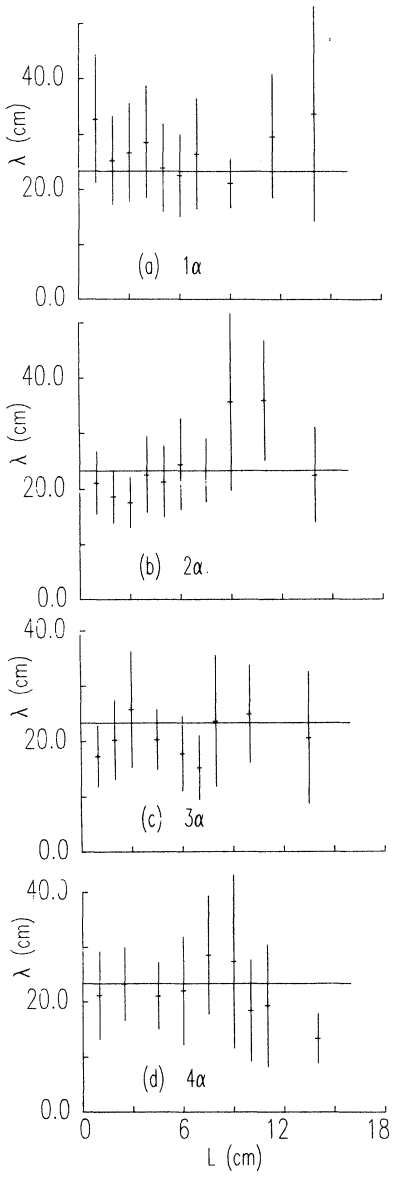

FIG. 1. Interaction mean free path λ as function of the distance L from the points of production for (a) 1α, (b) 2α, (c) 3α, and (d) 4α multiplicity events. The solid lines in these figures represent the overall mean free path of the helium fragments for the whole data sample.

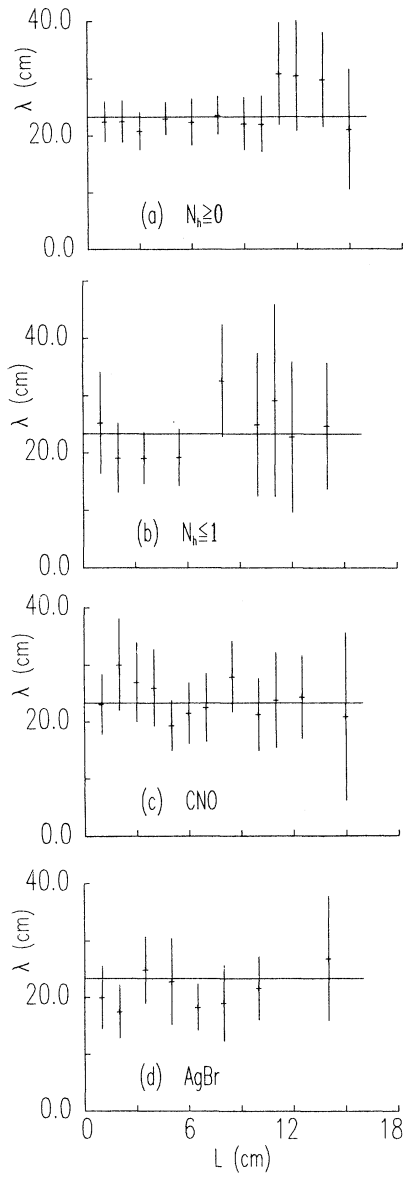

FIG. 2. Distribution of the mean free path λ in different path lengths L for (a) emulsion, (b) H, (c) CNO, and (d) AgBr targets of nuclear emulsion. The solid lines in these figures represent the overall mean free path of the helium fragments for the whole data set.

paths on the basis of different target sizes in the nuclear emulsion. This is shown in Figs. 2(a)–(d), where we plot λ vs L for the emulsion ($N_h \geq 0$), H ($N_h \leq 1$), CNO ($2 \leq N_h \leq 7$), and AgBr ($N_h \geq 8$) targets, respectively. The mean free paths do not depend upon the size of the target nucleus at the AGS energies. Average values of the interaction mean free paths for the H, CNO, and AgBr targets, within their statistical errors, are very close to the overall value of the mean free path of the whole data sample, $\lambda = 23.30 \pm 1.26$ cm (Table III). These findings confirm our previous results on the mean free paths of the projectile helium fragments at Bevatron and CERN energies.[4,5] However, our results on events with $N_h \leq 1$, just like at CERN energies,[4] are, once again, in contradiction to the results of Ghosh *et al.*[7] and El-Nadi *et al.*[8] The recent results of Khan *et al.*[9] agree with the observations of this experiment.

C. Multiplicity distributions of helium fragments

Finally, we discuss the multiplicity distribution of the helium fragments produced in the ^{28}Si-induced reactions at the AGS energies. In recent papers,[10,11] we reported the validity of the Koba-Nielsen-Olesen (KNO) scaling for projectile helium fragments produced from heavy-ion interactions at Bevatron and at CERN energies and here we are going to extend the KNO scaling at the AGS energies. As predicted by Koba, Nielsen, and Olesen,[12] multiplicity distributions $P(n)$ in high-energy collisions obey a scaling law

$$\psi(z) = \langle n_\alpha \rangle P(n_\alpha) = \langle n_\alpha \rangle \sigma_{n\alpha}/\sigma_{\text{inel}} , \quad (1)$$

which should be an energy-independent function of the scaled variable $z = n_\alpha / \langle n_\alpha \rangle$, where n_α represents the number of alpha particles produced in an event and $\langle n_\alpha \rangle$ is the average helium multiplicity of the whole data sample. σ_{inel} refers to the total inelastic cross section and $\sigma_{n\alpha}$ is the partial cross section for producing a state of multiplicity n_α. Another consequence of the multiplicity scaling implies the energy-independent moments

$$\langle n_\alpha^q \rangle / \langle n_\alpha \rangle^q = C_q . \quad (2)$$

In Refs. 10 and 11, it was shown that the multiplicity distributions of the produced helium fragments from the events of different projectiles over a wide range of energies can be represented by a universal function of the following form:

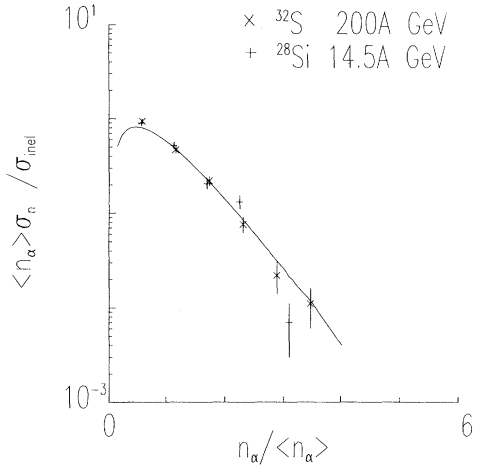

FIG. 3. The multiplicity distribution of $\langle n_\alpha \rangle \sigma_{n\alpha}/\sigma_{\text{inel}}$ as a function of the scaled variable $n_\alpha / \langle n_\alpha \rangle$ for the helium fragments. The solid curve represents the theoretical fitting of the data by a function given in Eq. (3).

$$\psi(z) = Az \exp(-Bz) , \quad (3)$$

where A and B are constants whose values are given in Ref. 10. In Fig. 3, we plot $\langle n_\alpha \rangle P(n_\alpha)$ as a function of the scaled variable $n_\alpha / \langle n_\alpha \rangle$ for the helium fragments emerged in ^{28}Si interactions. The data points for ^{28}Si at 14.5 A GeV and the ^{32}S at 200 A GeV data are represented by plus and cross symbols, respectively. In spite of the fact that the ^{28}Si projectile has energy less than that of the ^{32}S projectile by a factor of 14, all the data points (except for the last point of the ^{28}Si data due to its low statistics) for both of the projectiles lie on a simple universal curve represented by Eq. (3), suggesting a scaling behavior of multiplicity distributions of the helium fragments. In this experiment, the values of the constants are determined to be $A = 4.65 \pm 0.09$ and $B = 2.10 \pm 0.04$ with $\chi^2/\text{DF} = 0.003$, where DF represents degrees of freedom. Until now, we did not know the physical explanation of the helium multiplicity scaling and can perhaps regard it as an empirical observation.

Another way to test the validity of KNO scaling is to

TABLE IV. Average value of the helium multiplicty $\langle n_\alpha \rangle$, the C_q moments, and the ratio $\langle n_\alpha \rangle / D$.

Beam	Energy (A GeV)	$\langle n_\alpha \rangle$	C_2	C_3	C_4	C_5	$\langle n_\alpha \rangle / D$	Ref.
^{28}Si	14.5	1.78±0.08	1.30±0.06	2.11±0.09	3.96±0.17	8.24±0.36	1.82±0.08	This work
^{32}S	200	1.73±0.07	1.33±0.05	2.27±0.09	4.66±0.18	10.98±0.43	1.75±0.07	5
^{16}O	200	1.60±0.15	1.22±0.11	1.74±0.16	2.76±0.26	4.64±0.43	1.77±0.16	11
^{16}O	60	1.62±0.10	1.23±0.07	1.77±0.11	2.85±0.17	4.88±0.29	1.79±0.11	11
^{56}Fe	1.9	2.53±0.09	1.34±0.05	2.21±0.08	4.31±0.16	9.57±0.35	2.92±0.11	11
^{84}Kr	1.5	2.91±0.08	1.39±0.04	2.40±0.07	4.87±0.14	11.14±0.32	3.44±0.10	11
^{40}Ar	1.9	2.20±0.09	1.34±0.06	2.19±0.10			1.71±0.07	10

study the multiplicity distributions using C_q as given by Eq. (2). For the KNO scaling to be valid, the C_q moments should be energy independent and, therefore, in Table IV we present the results on the average multiplicities and the C_q moments for $q=2$, 3, 4, 5 of helium fragments produced in the interactions of ^{28}Si, ^{32}S, ^{16}O, ^{40}Ar, ^{56}Fe, and ^{84}Kr ions in emulsion at various incident energies. The C_2 and C_3 moments do not seem to depend upon the energy within the experimental errors; on the other hand, the higher moments show a slow increase in their values as the mass number (A) of the projectile increases. An interesting observation of this experiment is the value of the ratio $\langle n_\alpha \rangle / D$ for al the beams (Table IV), which is approximately equal to that observed in hadron-nucleus interactions. The variation of $\langle n_\alpha \rangle$ as a function of A is shown in Fig. 4, which can be approximately fitted by the following function:

$$\langle n_\alpha \rangle = a A^b , \quad (4)$$

where $a=0.56$ and $b=0.37$ with $\chi^2/\mathrm{DF}=0.05$. These values are approximately equal to those given in Refs. 10 and 11. It is worth mentioning that the average value of the helium multiplicity for the ^{28}Si and ^{32}S projectiles (Table IV) has remained almost constant over a wide range of energies for these two projectiles having almost the same masses.

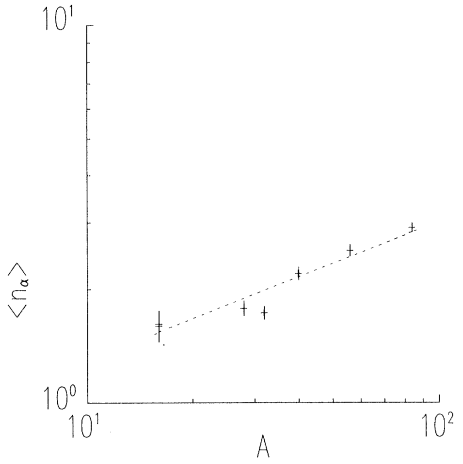

FIG. 4. A plot of average multiplicity $\langle n_\alpha \rangle$ vs the mass number A of the incident projectile. The dotted line represents a theoretical fitting of the data given by the functional form as employed in Eq. (4).

IV. CONCLUDING REMARKS

We conclude this study with the following remarks. The partial production cross sections σ_C and σ_P for the ^{28}Si and ^{32}S projectiles at $14.5A$ and $200A$ GeV are independent of energy for the projectiles having almost the same masses. This observation can be interpreted in terms of the geometry of collision at ultrarelativistic energies. This is also true for the partial cross sections of the multiple alpha emission channels for ^{28}Si and ^{32}S beams. The interaction mean free paths of the He fragments produced in collisions of ^{28}Si projectiles at the AGS energies are independent of the He multiplicity and the target size (emulsion, H, CNO, or AgBr). These findings corroborate our previous results on helium fragments produced at different energies with various incident heavy-ion projectiles.[4,5] The multiplicity distributions of the helium fragments produced in the ^{28}Si- and ^{32}S-induced emulsion reactions in the range of incident energies from $14.5A$ to $200A$ GeV exhibit a KNO scaling. The values of C_2 and C_3 moments are found to be independent of the masses and energies of the projectiles used in this work. The average multiplicity $\langle n_\alpha \rangle$ for the different projectiles at various incident energies can be parametrized in terms of the projectile mass A [Eq. (4)].

ACKNOWLEDGMENTS

We are thankful to Dr. D. Beavis, BNL, for his help in exposure and to Prof. G. Romano, CERN, for the development of our emulsion stack. This work was supported by Grant No. DE-FGO2-90ER40566.

*Present address: Daemen College, Amherst, NY 14226.

[1]K. Kajante, Proceedings of Quark Matter 88 [Nucl. Phys. **A498**, 355c (1989)], and the references therein.

[2]P. L. Jain, M. M. Aggarwall, and K. L. Gomber, Phys. Rev. C **34**, 726 (1986).

[3]A. Z. M. Ismail, M. S. El-Nagdy, K. L. Gomber, M. M. Aggarwal, and P. L. Jain, Phys. Rev. Lett. **52**, 1280 (1984); P. L. Jain, Nuovo Cimento **13**, 839 (1959).

[4]K. Sengupta, G. Singh, T. Ritter, and P. L. Jain, Europhys. Lett. **8**, 15 (1989); G. Singh, K. Sengupta, and P. L. Jain, Phys. Lett. B **214**, 480 (1988); P. L. Jain, K. L. Gomber, M. M. Aggarwal, and Vandana Rani, Phys. Lett. **154B**, 252 (1985).

[5]G. Singh, K. Sengupta, and P. L. Jain, Phys. Rev. C **42**, 1757 (1990).

[6]G. Singh, K. Sengupta, and P. L. Jain, Phys. Rev. C **41**, 999 (1990).

[7]D. Gosh, J. Roy, D. Banarjee, A. Dutta, R. Sengupta, K. Sengupta, K. Banarjee, and S. Naha, Phys. Rev. Lett. **54**, 396 (1985).

[8]M. El-Nadi, O. Badawy, A. Moussa, E. Khalid, and A. Hamalawy, Phys. Rev. Lett. **52**, 1971 (1984).

[9]M. Khan, M. Ahmed, K. Siddiqui, and R. Hasan, Nuovo Cimento **101**, 93 (1989).

[10]P. L. Jain and M. M. Aggarwal, Phys. Rev. C **33**, 1790 (1986).

[11]K. Sengupta, G. Singh, and P. L. Jain, Phys. Lett. B **222**, 301 (1989).

[12]Z. Koba, B. Nielsen, and P. Olesen, Nucl. Phys. **B40**, 317 (1972).